Effects of Higher-Order Multipoles on the Performance of a Two-Plate Quadrupole Ion Trap Mass Analyzer

Brett J. Hansen,[†] Hannah Quist, [†] Ying Peng, [‡] Zhiping Zhang,[‡] Junting Wang, [‡] Aaron R. Hawkins,[†] Daniel E. Austin[‡,*]

[†] Department of Electrical and Computer Engineering, Brigham Young University, Provo, Utah 84602

[‡] Department of Chemistry and Biochemistry, Brigham Young University, Provo, Utah 84602

*Corresponding author: austin@chem.byu.edu

Abstract

A simple method has been proposed to study the effects of multipole components on the performance of a radiofrequency quadrupole ion-trap mass analyzer, named the planar Paul trap. The device consists of two parallel ceramic plates, the opposing surfaces of which are lithographically imprinted with 24 metal rings. This suggested method combines the unique properties of this type of trap: the multiple-circular-ring structure, and ease of changing the electric field through differing capacitor configurations on printed circuit boards. Using this approach, the magnitude and sign of different multipole components, including octopole and dodecapole, can easily be adjusted through altering the voltage applied to each ring. This study presents a systematic investigation of the effects of multipole components (e.g., octopole and dodecapole) on the performance of the planar Paul trap. The results demonstrate that the octopole component has a more pronounced effect on the performance of the planar Paul trap than the dodecapole field, especially for ions with larger mass-to-charge ratios. Also, the sample concentration in the trapping region has a significant influence on the performance of the planar Paul trap with the change of the multipole components in trapping potentials.

1. Introduction

Over the past few decades ion trap mass spectrometers have found applications in a broad range of areas including physics,[1] biology,[2] environmental sciences,[3] and many others.[4, 5] In contrast to other types of mass analyzers (e.g., electric and magnetic sectors, time-of-flight), ion storage and confinement in an ion trap are accomplished using a time-dependent, radio-frequency (RF) electric field. By scanning the RF voltage or frequency, or by applying a supplemental ac signal, the trapped ions are ejected out of the confining electric field according to their different mass-to-charge ratios.[6]

During mass analysis, the mass resolution, sensitivity and mass measurement accuracy of an ion trap are strongly dependent on the contributions of higher-order components in the trapping field. Although an ideal quadrupole ion trap

contains only monopole and quadrupole potentials, all real electrode arrangements create higher-order multipole fields, such as octopole, dodecapole, etc. In commercial ion trap mass analyzers, performance is optimized by modifying the shape and/or arrangement of trap electrodes. For instance, the original Finnigan ion trap used additional space between electrodes, essentially "stretching" the trap by 10.8% in the axial direction. This modification changed the higher-order field components, and allowed much better performance than the unstretched version.[7] Bruker-Franzen instruments use an ion trap with a modified hyperbolic angle geometry.[8] To maximize the quadrupole field component relative to the higher-order field content, Wells et al.[10] optimized the geometry of a cylindrical ion trap through field calculations using the Poisson/Superfish code and through experimental variation of the electrode structure. In each case, changing the geometric structure of the trap introduces or modifies higher order components of the electric potential in the trapping region.[9] Numerous studies have examined the effect on higher-order multipoles resulting from geometric factors such as the endcap holes or apertures,[11-14] electrode alignment,[11,15-17] and electrode surface roughness.[18] It is difficult to eliminate higher-order components due to geometric factors in the fields of real traps.

Wu et al. studied the effects on the electric field of a cylindrical ion trap by changing its geometric structure.[15] Through geometric optimization, a "-10% compensation" criterion was suggested: the sum of octopole and dodecapole components should be -10% of the quadrupole component. Gill and co-workers investigated the effects of stretching and compressing the z_0 dimension of an ion trap via *in situ* optimization.[19] At the optimum stretch (~9%), both signal intensity and resolution were improved while mass accuracy was maintained.

Although geometry change is the most common approach to optimize the electric field in the trapping region, higher-order multipole components can also be modified by adding an ac signal, out of phase to each end cap, at the same frequency as the ring electrode. As reported by Splendore et al.,[20] the addition of a "trapping field dipole" component to the normal "stretched" ion trap hyperbolic electrode geometry would generate both a dipole and a significant hexapole component in the trapping field. With such fields the detected ion signal intensity was doubled and the mass resolution was improved.

Several software approaches have been employed to optimize the geometries of ion trap mass analyzers. All approaches include calculation of the multipole expansion of candidate trap geometries followed by optimization. The Cooks group has demonstrated this approach using a multi-particle trajectory simulation program, ITSIM.[15, 21, 22] After numerical computations of field composition, a few candidate geometries were manually selected using the "-10% compensation" criterion. Next, the ITSIM program was used to simulate the performance of the ion trap, and then experimental verification was carried out to identify the best geometry.[15] Another method, developed by Tallapragada et al.,[11] minimized the difference between the calculated and the desired multipole components to reach optimum geometry.[11, 23] SIMION 7.0 software[24] has also been used to determine the multipole expansion of a given electrode arrangement and geometry.[25] All of these approaches directly associate electrode geometry and field shape, and thus work within the constraints of electrode shape and position.

We have recently reported a new family of ion trap mass analyzers, including

the Halo ion trap[26] and the planar Paul trap.[27] Different from conventional ion traps, such as cylindrical, rectilinear, linear, and toroidal ion traps, that utilize metal electrodes to produce the appropriate electric fields, the trapping fields for our reported traps were realized by an array of metal electrode rings lithographically imprinted on ceramic disks.[26-28] The trapping fields in both traps were similar to those produced by shaped metal electrodes. In contrast to traps made using metal electrodes, the trapping fields in our devices can easily be adjusted by changing the voltages applied to different electrode rings, rather than by changing the geometries of the traps. The contribution of each multipole component (e.g., octopolar field and dodecapolar field) to the trapping field can be independently adjusted by changing the voltage to each ring. These devices allow study of the effects of higher-order field components on mass analysis. The present study examines the effects of higher-order field components on the performance of the planar Paul trap. Because the lowest even-order terms above quadrupole (i.e., octopole, dodecapole) are expected to have a larger effect on ion behavior than much higher terms (i.e., above 16-pole), this study focuses on these lower terms.

2. EXPERIMENTAL SECTION

2.1 Optimization methodology

The device used in the present study consisted of an assembly of two plates. One surface of each plate was lithographically patterned with 24 metal rings, as illustrated in Figure 1. The dimensions of the device and locations of the rings were given previously.[27] Because the outer rings did not make a significant contribution to the electric potential at the trap center, only the first 11 rings were used in the present study. The outer 13 rings were electrically shorted to ring 11. The 1st and 24th rings were grounded in simulations, constrained by the design of the printed circuit boards (PCBs). The remaining rings were connected to capacitors in an RF capacitive voltage divider, located on printed circuit boards behind each patterned plate. The RF amplitude on each ring is determined by the choice of capacitor value associated with that ring.

SIMION and MATLAB were used to calculate the multipole expansion corresponding to each ring electrode, using an approach similar to that of Chaudhary.[25] Specifically, SIMION potential arrays were set up for each ring (with all other rings at zero). A neutron was "flown" through the center of the trap along the *z*-axis ($r = 0$), and the potential recorded at each step. These potential values were imported into MATLAB and a least-squares fit of the nominally quadratic electric potential was calculated. Determination of the multipoles with the least-squares fit in MATLAB R2008b was performed as a polynomial with up to 20 poles to obtain the desired degree of accuracy for the lower order multipoles.

As demonstrated in recent work,[29] the multipole components in the electric field of this type of trap can be approximately obtained by adding the multipole component contributions of each individual ring. By the superposition principle, the multipole expansion of the entire trap is the sum of the normalized multipole expansion contributed by each individual ring electrode, weighted by the RF amplitude applied to that ring:

$$A_2 \approx \sum_{ring=2}^{ring=11-23} (V_{ring(i)} \cdot A_{2,ring(i)})$$

$$A_4 \approx \sum_{ring=2}^{ring=11-23} (V_{ring(i)} \cdot A_{4,ring(i)})$$

$$A_6 \approx \sum_{ring=2}^{ring=11-23} (V_{ring(i)} \cdot A_{6,ring(i)})$$

where $V_{ring(i)}$ is the voltage applied to ring i; $A_{2,ring(i)}$, $A_{4,ring(i)}$, and $A_{6,ring(i)}$ are the normalized contributions of quadrupolar field, octopolar field, and dodecapolar field for ring i; and A_n is the multipole term for the entire device.

The RF amplitudes for each ring, and the corresponding capacitor values, were determined using the Solver function in Microsoft Excel. With this method, one can calculate the percentages of A_4/A_2 and A_6/A_2 if the voltages applied to different rings are known, and also calculate the voltages to different rings if the percentages of A_4/A_2 and A_6/A_2 are fixed. For example, the targeted percentages for octopolar field and dodecapolar field are, respectively, 2.0% and 4.0%. In this calculation, the individual ring voltages are set as variables, and the results of multiplying the normalized voltages by quadrupolar field ($A_{2,\ ring(i)}$), octopolar field ($A_{4,\ ring(i)}$), and dodecapolar field ($A_{6,\ ring(i)}$) from each ring are set as constants. The SOLVER function in Microsoft Office Excel is then used to solve for the voltages to the different rings. Finally, the corresponding capacitors for the voltage divider circuit on the PCBs can be obtained. Several combinations of octopole and dodecapole (for the entire device) were chosen for the present study.

2.2 Experimental verification

The performance of the planar Paul trap with different electric fields was tested in an instrumental setup as described previously.[27] The setup includes an electron gun assembly, trapping region, and an electron multiplier detector. Behind each of the two ceramic plates comprising the trapping region was a PCB with a capacitor network. The capacitor network was used to establish the voltages on each of the ring electrodes under RF excitation. Spring-loaded pins were soldered to the PCBs in order to make electrical contact with the back sides of the trapping plates. A 6-mm stainless steel spacer was mounted between the trapping plates. Holes in the spacer admitted the electron beam, sample vapor, helium gas, and a Teflon tube leading to a pirani gauge (Kurt J. Lesker, Clairton, CA). An RF signal with a frequency of 1.26 MHz and variable amplitude up to 738 $V_{0\text{-}p}$ (PSRF-100, Ardara Technologies, North Huntingdon, PA) was applied to the capacitor network on the PCBs, and the spacer was grounded during ion ejection. In addition, a supplementary low-voltage ac signal, generated using a 30 MHz synthesized function generator (DS345, Stanford Research Systems, Sunnyvale, CA) and a converter having two outputs with 180^o phase difference, and amplified to 0.7 $V_{0\text{-}p}$ and 1.5 $V_{0\text{-}p}$ by a custom-made amplifier, was applied between the trapping plates to provide a dipole field for resonant ion ejection during the RF scan. The amplified supplementary ac signals were applied to the innermost ring on each plate, using a simple filter circuit to isolate the supplementary ac from the main RF signals. The applied frequency of the ac signal was 345 kHz, and β_z was approximately 0.55. The operational details of the planar Paul ion trap are similar to those described in our recent study.[27] An electron multiplier detector (DeTech Detector Technology), Inc., Palmer, MA) was used to detect the ejected ions, with a detector voltage operated at -1,650 V. The signal was amplified (427 Current Amplifer, Keithley Instruments, Cleveland, OH) and recorded using a digital oscilloscope (WaveRunner 6000A, LeCroy, Chestnut Ridge, NY).

For all experiments, helium was used as the buffer gas at an indicated pressure of 5.34×10^{-3} Torr (uncorrected, 1 Torr = 133 Pa) as read from the pirani gauge. Headspace vapor of the organic compounds of interest, without further purification, was leaked into the vacuum through two

Swagelok leak valves (Swagelok, Solon, OH) to maintain a nominal pressure of 1.0-8.0 × 10^{-5} Torr. In situ electron ionization was achieved using a custom-built electron gun comprising an iridium-filament, lens, gate, and a 1.6-amp power supply.

3. RESULTS AND DISCUSSION

3.1 Performance comparison of the planar Paul trap with 2.0% octopole + 8.0% dodecapole, and with 8.0% octopole + 2.0% dodecapole

In an ion trap, the quadrupolar field (A_2), octopolar field (A_4), and dodecapolar field (A_6) have the most crucial role among the multipole expansion coefficients. Therefore, only the influence of octopole and dodecapole components on the performance of the planar Paul trap was investigated in this work. In order to obtain the optimum performance of an ion trap mass analyzer by altering its electric field, it is important to know what range of multipole components will produce the optimum electric field. Electric fields with 2.0% octopole and 8.0% dodecapole, and with 8.0% octopole and 2.0% dodecapole were first investigated. Figure 2 demonstrates the spectra of acetone and dichloromethane using trapping fields with 2.0% octopole and 8.0% dodecapole, and with 8.0% octopole and 2.0% dodecapole. By comparing both spectra, it can be seen that the resolution (full-width-at-half-maximum, FWHM) for the *m/z* 58 ion of acetone and the *m/z* 84 ion of dichloromethane from the electric field with 2.0% octopole and 8.0% dodecapole are 85 and 93, respectively, while the resolution for the same peaks are 54 and 59 for the field with 8.0% octopole and 2.0% dodecapole. In addition, the signal-to-noise ratios for the former are 21.9 and 11 respectively, whereas the values for the latter are only 4.7 and 2.6. These results suggest that the electric field with 2.0% octopole and 8.0% dodecapole is superior to that with 8.0% octopole and 2.0% dodecapole for the present trap.

3.2 Performance comparison of the planar Paul trap with different signs of octopole and dodecapole

As reported by Wu et al., the optimum performance of a cylindrical ion trap was obtained when the sum of the relative strengths for the positive octopolar field and the negative dodecapolar field was about -10%.[15] By optimizing the geometry of the rectilinear ion trap, Ouyang et al. also found that when the sum of octopole and dodecapole components was about -10%, the trap demonstrated good performance.[30] However, Tallapragada and co-workers[11] regarded the "-10% compensation" rule as a compromise result. After geometry optimization of a cylindrical ion trap with BEM method, which possessed the same geometry as that of Wu et al.,[15] they concluded that when the octopole and dodecapole components (namely, A_4/A_2 and A_6/A_2) were respectively 96.1% and 0.3%, the trap showed good performance.

To comprehensively investigate the effect of octopole and dodecapole electric field strengths on the performance of the new trap, electric fields with the same magnitude but different signs of octopole and dodecapole components were investigated. From the above section, it is obvious that the electric field with 2.0% octopole and 8.0% dodecapole demonstrates a better performance relative to that with 8.0% octopole and 2.0% dodecapole. The octopole contribution is generally the strongest and most essential of the even-order multipole fields in a quadrupole ion trap.[31] In consideration of this point, we used an intermediate value of the above dodecapole component at 4.0%, while

keeping the octopole component of 2.0% constant in the following study. Figure 3 shows the performance of the planar Paul trap with all combinations of ±2.0% octopole and ±4.0% dodecapole.

Figure 3(a) demonstrates the comparison of resolution (FWHM) for the *m/z* 78 Th ion of benzene, the *m/z* 84 Th ion of dichloromethane, the *m/z* 91 Th ion of toluene, and the *m/z* 134 Th ion of butylbenzene under different octopolar and dodecapolar fields. The experiments were carried out individually. The electric fields with ±2.0% octopole and -4.0% dodecapole give similar performance for all ions studied. The mass resolution for these experiments is in the range of 140-300. In addition, the value gradually increases with the increase of mass-to-charge ratio except for the *m/z* 84 Th ion of dichloromethane under 2.0% octopole and -4.0% dodecapole. Namely, the *m/z* 78 Th ion of benzene shows the lowest resolution, while the *m/z* 134 Th ion of butylbenzene demonstrates the highest. For the electric fields with ±2.0% octopole and 4.0% dodecapole, the performances have a similar pattern, and the resolution changes dramatically with the increase of *m/z*. For example, under the electric field of 2.0% octopole and 4.0% dodecapole, the resolution for the *m/z* 78 Th ion of benzene was 173, then it increased to 228 for *m/z* 84 followed by decreasing to 127 for *m/z* 91 Th. With the further increase of *m/z* up to 134 Th, the value decreased to 41. From this figure it can be seen that the electric fields with ±2.0% octopole and -4.0% dodecapole show a better performance for all the compounds studied.

Signal-to-noise ratio (S/N) is another important parameter to evaluate the performance of an ion trap. It is well-known that the signal strength increases with an increase of ionization time over a certain range. For comparing the S/N of the investigated ions for the same conditions of octopole and dodecapole components in the trapping field, the signal strength values have been normalized with the ionization time. Explicitly, the S/N shown in Figure 3(b) is the S/N value divided by its corresponding ionization time. As shown in Figure 3(b), for electric fields with ±2.0% octopole & and -4.0% dodecapole, the S/N first increases, followed by a decrease with the increase of *m/z*. For example, when the electric field contained 2.0% octopole and -4.0% dodecapole, the S/N for *m/z* 78 Th was 1.67, and then 3.00 for *m/z* 84 Th. With the increase of *m/z*, the value decreased to 1.02, and further increasing *m/z* up to 134 led to an S/N of 0.85. However, the S/N from ±2.0% octopole and 4.0% dodecapole has another pattern. The S/N gradually decreased with the increase of *m/z* although there was some exception for *m/z* 84 Th ion of dichloromethane in the electric field with -2.0% octopole and 4.0% dodecapole. Specifically, the *m/z* 78 Th ion of benzene illustrates the largest S/N, and the *m/z* 134 Th ion of butylbenzene shows the lowest. As a whole, for all the compounds studied, 2.0% octopole and 4.0% dodecapole gives the lowest S/N values, whereas the S/N is comparable for the other three electric fields.

In the present study, we also found that the sample concentration in the trapping region had a large impact on performance. For example, when the headspace vapor of organic compounds was injected through a Teflon tube directly into the trapping field between the two ceramic plates, some lower *m/z* ions were not observed. However, when the headspace vapor of the organic compounds was injected into the vacuum system without the Teflon tube, a strong signal from the lower *m/z* ions appeared and the resolution increased. Figure 4 shows the spectra of dichloromethane and toluene under both conditions. From Figure 4(a), it is obvious that when the sample was directly

injected into the trapping region, only a tiny *m/z* 49 Th peak was observable for dichloromethane. In contrast, two intense peaks (*m/z* 49 Th and *m/z* 51 Th) can be observed when the sample was directly injected into the vacuum system rather than the trapping region (Figure 4(b)). Peak resolution also increased in the latter case. For example, the resolution for *m/z* 84 Th was only 135 when dichloromethane was directly injected into the trapping region, but increased to 274 when injected into the vacuum system. For the case of toluene, as shown in Figure 4(c) and (d), the same phenomenon was also observed.

Peak intensity and resolution may be correlated with sample concentration in the trapping region. When the headspace vapor of the studied samples was directly injected into the trapping region, the neutral sample gas density increases and more collisions between the ions and neutral gas molecules will occur. This explains why the products of ion-molecular ions, such as *m/z* 105 Th, were observed, as shown in Figure 4(c) and (d). This assumption can be confirmed by the more intensive peak of *m/z* 105 Th in Figure 4(c) than that in Figure 4(d). Due to ion-molecule reactions, the molecular ions are less likely to fragment, and the ratio of ion-molecular ions to lower *m/z* ions increases. At the same time, the space charge effect between them increases and the resolution deteriorates. Doroshenko and Cotter attributed ion losses to a nonlinear resonance due to the weak octopole field in the trap, and it was possible to avoid such losses during reverse scans at relatively fast scan rates,[31] in agreement with our recent study during forward scans.[27] The above results, to a certain degree, suggest that the sample concentration in the trapping region has an effect on the multipole components (e.g., octopole) and, therefore, influence of ejection of the lower *m/z* ions.

Additional results showing the dependence on injection location are shown in Figure 3(c) and (d) for electric fields with ±2.0% octopole and ±4.0% dodecapole. From Figure 3(c), it is obvious that with the increase of *m/z*, there is no clear trend for resolution under the studied electric fields; however there are some cases that highlight the differences in injection location. For example, for *m/z* 134 Th and ±2.0% octopole and 4.0%, the value in Figure 3(a) is in the range of 41-55 – representing injection in the trap region. In Figure 3(c) (representing injection only into the vacuum system) the resolution for ±2.0% octopole and 4.0% dodecapole increased as high as 260 and 685. As mentioned above, the lower resolution in Figure 3(a) is attributable to the high concentration of butylbenzene in the trapping region.

Signal to noise ratio also shows some dependence on sample injection location. In general we see a decrease of S/N with the increase of *m/z*. This may be attributable to the different scan speeds used for the different species [benzene (661.30 Th/s) < dichloromethane (1174.93 Th/s) > toluene (417.20 Th/s) > butylbenzene (412.06 Th/s)] and different ionization energies [benzene (9.24 eV) < dichloromethane (11.33 eV) > toluene (8.83 eV) > butylbenzene (8.69 eV)]. By comparing the graphs in Figure 3, it is obvious that the performance of the trap (e.g., resolution and S/N) is comparable for the electric fields of ±2.0% octopole and -4.0% dodecapole when injecting into the trapping region between the two plates and into the vacuum system. However, the performance for ±2.0% octopole and 4.0% dodecapole changes significantly.

3.3 Performance comparison of the planar Paul trap with different percentages of octopole while keeping dodecapole component constant

Figure 5 shows the effect of the octopole component on the resolution for the *m/z* 49, 84, and 86 Th ions of dichloromethane, and the 130 and 132 Th ions of trichloroethylene while keeping -4.0% dodecapole constant. These experiments were carried out individually when the headspace vapor of the organic compounds was injected into the trapping field between the two ceramic plates through a Teflon tube and injected directly into the vacuum system. It is evident in Figure 5 that with the increase of octopole component from -8.0% to 8.0%, the resolution for all investigated ions has a similar trend. When the octopole component was 0.0%, the resolutions show their highest values. Moreover, the resolution increases with the increase of *m/z*. For example, in Figure 5(b) the resolution was only 110 for *m/z* 49 Th when 0.0% octopole component was added into the electric field. This value increased to 415 for *m/z* 132 Th. By comparing Figure 5(a) with Figure 5(b), it can also be seen that changing the injection location did not significantly affect the resolution of the lower *m/z* ions (e.g., 49 Th, 84 Th, and 86 Th), although the value for the higher *m/z* ions (e.g., 130 Th and 132 Th) did increase. For example, in Figure 5(a), the resolution for *m/z* 130 Th was 301 when 0.0% octopole component was added into the trapping field, and this value became 432 in Figure 5(b).

Figure 5 also makes clear that large negative octopole components (-8.0% to -4.0%) are more beneficial to resolution than large positive octopole components (8.0% to 4.0%). This is related to the report by Franzen et al.,[32] which shows that with positive octopole field superposition, an ion took up energy from the RF drive field as soon as its working point crossed the stability boundary, increasing its secular oscillation amplitude exponentially, and almost immediately being ejected. In contrast, with negative octopole fields, the ion ejection was delayed. Therefore, the negative octopoles were responsible for a poor mass resolution, whereas positive octopoles favored a good resolution. The above reasoning would contradict our data. To our knowledge, the difference between the report of Franzen et al. and our results can be attributed to the different ejection modes and the contribution of other multipoles (e.g., hexadecapole (A_8), ikosipole (A_{10}), and tetraikosipole (A_{12})). For this study, dipole resonant ejection was used whereas boundary ejection was used in the Franzen study. In the present study, the relative values of hexadecapole (A_8/A_2), ikosipole (A_{10}/A_2), and tetraikosipole (A_{12}/A_2) are much larger than that of octopole (A_4/A_2), as listed in Table 1, while in the Franzen study these larger order pole contributions were relatively small compared to the octopole. Table 1 also shows that with the decrease of octopole components from 8.00% to -8.00% while keeping the dodecapole constant, hexadecapole (A_8/A_2) and tetraikosipole (A_{12}/A_2) components gradually increased from -42.23% to -28.66%, and -312.51% to -254.91%, respectively. Therefore, the negative octopole component was compensated by other multipole components (e.g., A_8/A_2 and A_{10}/A_2). This fact, to some extent, accounts for why negative octopole components favored a better resolution in the present study.

3.4 Performance comparison of the planar Paul trap with different percentages of dodecapole while keeping octopole component constant

To study the effect of the dodecapolar field on the performance of the planar Paul trap, experiments were carried out in which the dodecapole component of the trapping field ranged from -6.0% to 12.0%, while

keeping the octopole component at 0.0%. Figure 6 shows the resolution trend for the *m/z* 49, 84, and 86 Th ions of dichloromethane, and 130 and 132 Th molecular ions of trichloroethylene. From this figure it can be seen that as the dodecapole changes, the resolution increases with increasing *m/z,* although there is some exception for 8.0% in Figure 6(a) and for 12.0% in Figure 6(b). Also, similar to the trend in Figure 5, the resolution determined by the *m/z* 86 Th and 132 Th ions is a little lower than their corresponding isotopic ions *m/z* 84 Th and 130 Th in some cases. More importantly, when the headspace vapor of the organic compounds was directly injected into the trapping field between the two ceramic plates through a Teflon tube, the resolution keeps almost constant excluding the 6.0% dodecapole, as shown in Figure 6(a). However, when the Teflon tube was removed from the system, the resolution demonstrates a gradually increasing trend with the increase of dodecapole component from -6.0% to 8.0%, followed by decreasing resolution with further increases in the percentage of dodecapole (Figure 6(b)). These results illustrate that the performance of the present planar Paul trap is very sensitive to the change of dodecapole component at a low sample concentration in the trapping region. On the other hand, when the sample was directly injected into the trapping region between the two ceramic plates, the resolution remained almost constant with change of the dodecapole percentage in the electric field. This observation suggests that at a higher sample concentration in the trapping region, the change of the dodecapole component has little effect on the performance of the trap.

As stated above, when the headspace vapor of the studied sample was injected directly into the trapping region, an overall reduction in performance was observed due to a pronounced space charge effect resulting from a higher sample concentration in the trapping region. As reported by Schwartz et al. [33] the space charge effect can significantly limit the performance (e.g., resolution, mass accuracy, sensitivity, and dynamic range) of all ion trap mass spectrometers. For the present case, the small influence of the dodecapole component on the resolution of the trap could also be attributed to the space charge effect. Specifically, when the number of the trapped ions, especially the molecular ions or the ions resulting from ion-molecule reactions, is large enough, space charge will dominate performance. Also, in contrast to the quadrupole field and octopole field, the dodecapole component makes little contribution to the overall electric field. Therefore, the space charge effect will outweigh the change of dodecapole component ranging from -6.0% to 12.0%, and the resolution for the studied ions kept almost constant in this range. When the sample concentration in the trapping region is lower, as is the case without direct vapor injection, the effect of dodecapolar field is more significant than the space charge effect. Thus a gradual change in the resolution appeared with the change of dodecapole component.

Mass resolution in ion trap mass analyzers is dependent on the scan speed[27, 30, 34-36] and scan mode,[37-39] and this has also been observed in the present system. It is important to note that the above experiments were carried out at an intermediate scan speed and forward scan, which is not expected to yield the highest resolution possible. Mass resolution as high as 1,100 has been observed for a slower scan speed (412.06 Th/s) and reverse scan in the Planar Paul trap. An example of a higher-resolution spectrum taken with this device is shown in Figure 7.

Conclusions

The optimization of electric fields in a planar Paul trap can be easily achieved by manipulating the voltages applied to discrete ring electrodes. For this approach, the contribution of the multipole components (e.g., quadrupole, octopole, dodecapole, and so on) from different electrodes was first obtained through the ion optical simulation program SIMION and an equation solver. Target voltages were obtained by constructing a capacitor network on a printed circuit board and connecting it to plates containing the trap's ring electrodes. Experimental demonstrations of the effects of octopole and dodecapole components on the performance of the planar Paul trap have been presented and suggest that significant improvements to resolution and signal-to-noise ratio can be. It is believed that a similar optimization procedure can be extended to the electric fields of other ion traps, such as the conventional Paul trap, cylindrical ion trap, linear ion trap, and those being developed by our research group.

ACKNOWLEDGMENT

This work was supported by the NASA Planetary Instrument Definition and Development Program, NNH06ZDA001N. We also gratefully acknowledge many helpful discussions with Dr. Wei Xu in Purdue University on calculations of multipole components.

REFERENCES

(1) Maiwald, R.; Leibfried, D.; Britton, J.; Bergquist, J. C.; Leuchs, G.; Wineland, D. J. *Nature Phys.* **2009**, *5*, 551-554.

(2) Wu, H. Y.; Tseng, V. S. M.; Chen, L. C.; Chang, Y. C.; Ping, P. P.; Liao, C. C.; Tsay, Y. G.; Yu, J. S.; Liao, P. C. *Anal. Chem.* **2009**, *81*, 7778-7787.

(3) Gros, M.; Petrovic, M.; Barcelo, D. *Anal. Chem.* **2009**, *81*, 898-912.

(4) Hiura, H.; Kanayama, T. *J. Mol. Struct.* **2005**, *735*, 367-374.

(5) Wold, C.; van de Grampel, R. *Polymer Test.* **2009**, *28*, 495-499.

(6) Williams, S. M.; Siu, K.W. M.; Londry, F. A.; Baranov, V. I. *J. Am. Soc. Mass Spectrom.* **2007**, *18*, 578-587.

(7) Stafford, G. C.; Kelley, P. E.; Stephens, D. R. U.S. Patent 6,540,884, 1985.

(8) Sudakov, M. *Int. J. Mass Spectrom.* **2001**, *206*, 27-43.

(9) March, R. E.; Londry, F. A.; Alfred, R. L. *Org. Mass Spectrom.* **1992**, *27*, 1151-1152.

(10) Wells, J. M.; Badman, E. R.; Cooks, R. G. *Anal. Chem.* **1998**, *70*, 438-444.

(11) Tallapragada, P. K.; Mohanty, A. K.; Chatterjee, A.; Menon, A. G. *Int. J. Mass Spectrom.* **2007**, *264*, 38-52.

(12) Koizumi, H.; Whitten, W. B.; Reilly, P. T. A.; Koizumi, E. *Int. J. Mass Spectrom.* **2009**, *281*, 108-114.

(13) Chattopadhyay, M.; Verma, N. K.; Mohanty, A. K. *Int. J. Mass Spectrom.* **2009**, *282*, 112-122.

(14) Chattopadhyay, M.; Mohanty, A. K. *Int. J. Mass Spectrom.* **2009**, *288*, 58-67.

(15) Wu, G.; Cooks, R. G.; Ouyang, Z. *Int. J. Mass Spectrom.* **2005**, *241*, 119-132.

(16) Blain, M. G.; Riter, L. S.; Cruz, D.; Austin, D. E.; Wu, G.; Plass, W. R.; Cooks, R. G. *Int. J. Mass Spectrom.* **2004**, *236*, 91-104.

(17) Chaudhary, A.; van Amerom, F. H. W.; Short, R. T.; Bhansali, S. *Int. J. Mass Spectrom.* **2006**, *251*, 32-39.

(18) Xu, W.; Chappell, W. J.; Cooks, R. G.; Ouyang, Z. *J. Mass Spectrom*. **2009**, *44*, 353-360.

(19) Gill, L. A.; Amy, J. W.; Vaughn, W. E.; Cooks, R. G. *Int. J. Mass Spectrom.* **1999**, *188*, 87-93.

(20) Splendore, M.; Marquette, E.; Oppenheimer, J.; Huston, C.; Wells, G. *Int. J. Mass Spectrom.* **1999**, *190/191*, 129–143.
(21) Bui, H. A.; Cooks, R. G. *J. Mass Spectrom*. **1998**, *33*, 297-304.
(22) Plass, W. R. Ph.D. Thesis, Justus-Liebig-Universität Gießen, Germany, 2001.
(23) Krishnaveni, A.; Verma, N. K.; Menon, A. G.; Mohanty, A. K. *Int. J. Mass Spectrom.* **2008**, *275*, 11-20.
(24) Dahl, D. A. *Int. J. Mass Spectrom.* **2000**, *200*, 3-25.
(25) Chaudhary, A.; van Amerom, F. H. W.; Short, R. T.; Bhansali, S. *Int. J. Mass Spectrom.* **2006**, *251*, 32-39.
(26) Austin, D. E.; Wang, M.; Tolley, S. E.; Maas, J. D.; Hawkins, A. R.; Rockwood, A. L.; Tolley, H. D.; Lee, E. D.; Lee, M. L. *Anal. Chem.* **2007**, *79*, 2927-2932.
(27) Zhang, Z.; Peng, Y.; Hansen, B. J.; Miller, I. W.; Wang, M.; Lee, M. L.; Hawkins, A. R.; Austin, D. E. *Anal. Chem.* **2009**, *81*, 5241-5248.
(28) Austin, D. E.; Peng, Y.; Hansen, B. J.; Miller, I. W.; Rockwood, A. L.; Hawkins, A. R.; Tolley, S. E. *J. Am. Soc. Mass Spectrom.* **2008**, *19*, 1435-1441.
(29) Austin, D. E.; Hansen, B. J.; Peng, Y.; Zhang, Z. Submitted to *Int. J. Mass Spectrom*. **2010**.
(30) Ouyang, Z.; Wu, G.; Song, Y.; Li, H.; Plass, W. R.; Cooks, R. G. *Anal. Chem.* **2004**, *76*, 4595-4605.
(31) Doroshenko, V. M.; Cotter, R. J. *J. Am. Soc. Mass Spectrom.* **1997**, *8*, 1141-1146.
(32) Franzen, J.; Gabling, R.-H.; Schubert, M.; Wang, Y. In *Practical Aspects of Ion Trap Mass Spectrometry*; March, R. E., Todd, J. F. J., Eds.; CRC Press: New York, USA, 1995; Vol. 1, pp 49-167.
(33) Schwartz, J. C.; Senko, M. W.; Syka, J. E. P. *J. Am. Soc. Mass Spectrom.* **2002**, *13*, 659-669.
(34) Schwartz, J. C.; Syka, J. E. P.; Jardine, I. *J. Am. Soc. Mass Spectrom.* **1991**, *2*, 198–204.
(35) Kaiser, R. E.; Cooks, R. G.; Stafford, G. C.; Syka, J. E. P.; Hemberger, P. H. *Int. J. Mass Spectrom. Ion Process.* **1991**, *106*, 79–115.
(36) Williams, J. D.; Cox, K.; Morand, K. L.; Cooks, R. G.; Julian, R. K., Jr.; Kaiser, R. E. In *Proceedings of the 39th Annual Conference of Mass Spectrometry and Allied Topics*, Nashville, TN, 1991; p 1481.
(37) Wells, J. M.; Plass, W. R.; Cooks, R. G. *Anal. Chem.* **2000**, *72*, 2677-2683.
(38) Williams, J. D.; Cox, K. A.; Cooks, R. G.; McLuckey, S. A.; Hart, K. J.; Goeringer, D. E. *Anal. Chem.* **1994**, *66*, 725–729.
(39) Dobson, G.; Murrell, J.; Despeyroux, D.; Wind, F.; Tabet, J.-C. *Rapid Commun. Mass Spectrom.* **2003**, *17*, 1657-1664.

Captions to Figures and Tables

Figure 1. Structure of the ceramic plate for the planar Paul trap.

Figure 2. Comparison of mass spectra of (a) acetone and (b) dichloromethane under 2.0% octopolar field and 8.0% dodecapolar field, and 8.0% octopolar field and 2.0% dodecapolar field. Ions were ejected using a supplementary dipole amplitude of 1.5 $V_{0\text{-}p}$ and frequency of 445 kHz.

Figure 3. Comparison of resolution (FWHM) [(a) and (c)] and signal-to-noise ratio [(b) and (d)] for the *m/z* 78 Th ion of benzene, the *m/z* 84 Th ion of dichloromethane, the *m/z* 91 Th ion of toluene, and the *m/z* 134 Th ion of butylbenzene under different octopolar and dodecapolar fields. These values are from individual spectra. Note: (a) and (b): headspace vapor of the organic compounds was injected into the trapping field between two ceramic plates through a Teflon tube; (c) and (d): headspace vapor of the organic compounds was injected into the vacuum system without Teflon tube. Each data point represents the average of three measurements. The signal-to-noise was normalized to the corresponding ionization time.

Figure 4. Comparison of mass spectra of dichloromethane [(a) and (b)] and toluene [(c) and (d)] under dipole ejection conditions: (a) and (c) headspace vapor of the organic compounds was injected into the trapping field between two ceramic plates through a Teflon tube, and (b) and (d) headspace vapor of the organic compounds was injected into the vacuum system without Teflon tube. Other conditions: ac frequency: 345 kHz, amplitude: 0.7 $V_{0\text{-}p}$, Ionization time: (a) 6.0 ms, (b) 10.0 ms, (c) 6.0 ms, and (d) 16.0 ms.

Figure 5. Comparison of resolution (FWHM) for the *m/z* 49, 84, and 86 ions of dichloromethane, and the *m/z* 130 and 132 Th ions of trichloroethylene using different octopolar field, while keeping the dodecapole percentage at -4.0 %. These values are from individual spectra. (a) Headspace vapor of the organic compounds was injected into the trapping field between two ceramic plates through a Teflon tube, and (b) headspace vapor of the organic compounds was injected into the vacuum without Teflon tube. Each data point represents the average of three measurements.

Figure 6. Comparison of resolution (FWHM) for the *m/z* 49, 84, and 86 Th ions of dichloromethane, and the *m/z* 130 and 132 Th ions of trichloroethylene under different dodecapolar field while keeping the octopole constant at 0.0%. These values are from individual spectra. (a) Headspace vapor of the organic compounds was injected into the trapping field between two ceramic plates through a Teflon tube, and (b) headspace vapor of the organic compounds was injected into the vacuum without Teflon tube. Each data point represents the average of three-time measurements.

Figure 7. Mass spectrum of butylbenzene. Other conditions: ac frequency: 330 kHz; amplitude: 1.0 $V_{0\text{-}p}$; ionization time: 0.2 ms; scan mode: reverse scan.

Table 1. The relative weights of multipoles including octopole (A_4/A_2), dodecapole (A_6/A_2), hexadecapole (A_8/A_2), ikosipole (A_{10}/A_2), and tetraikosipole (A_{12}/A_2) used in each experiment.

Figure 1

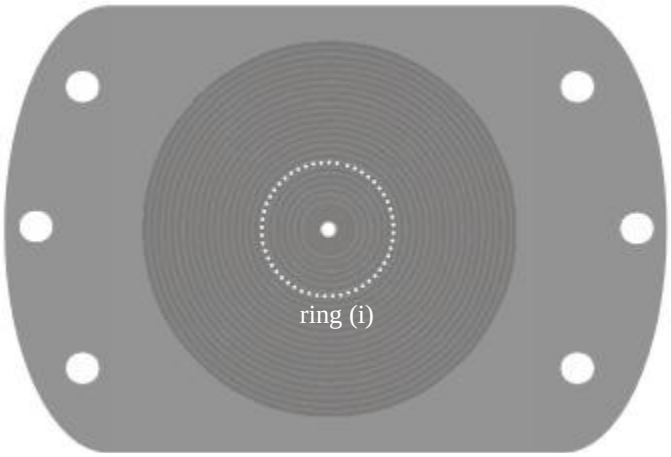

Figure 2

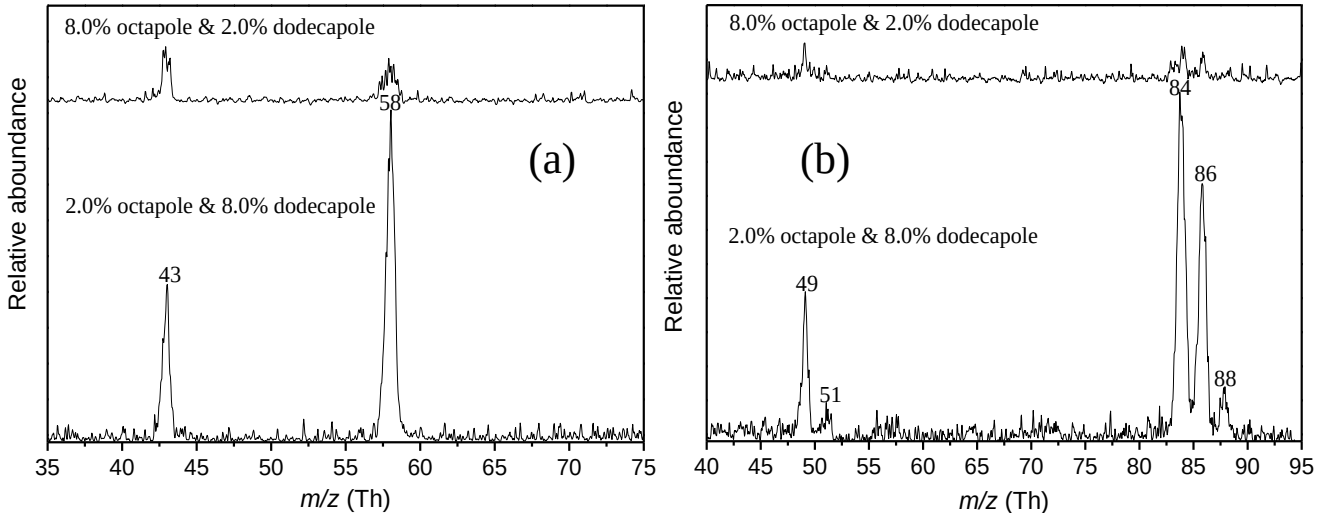

Figure 3

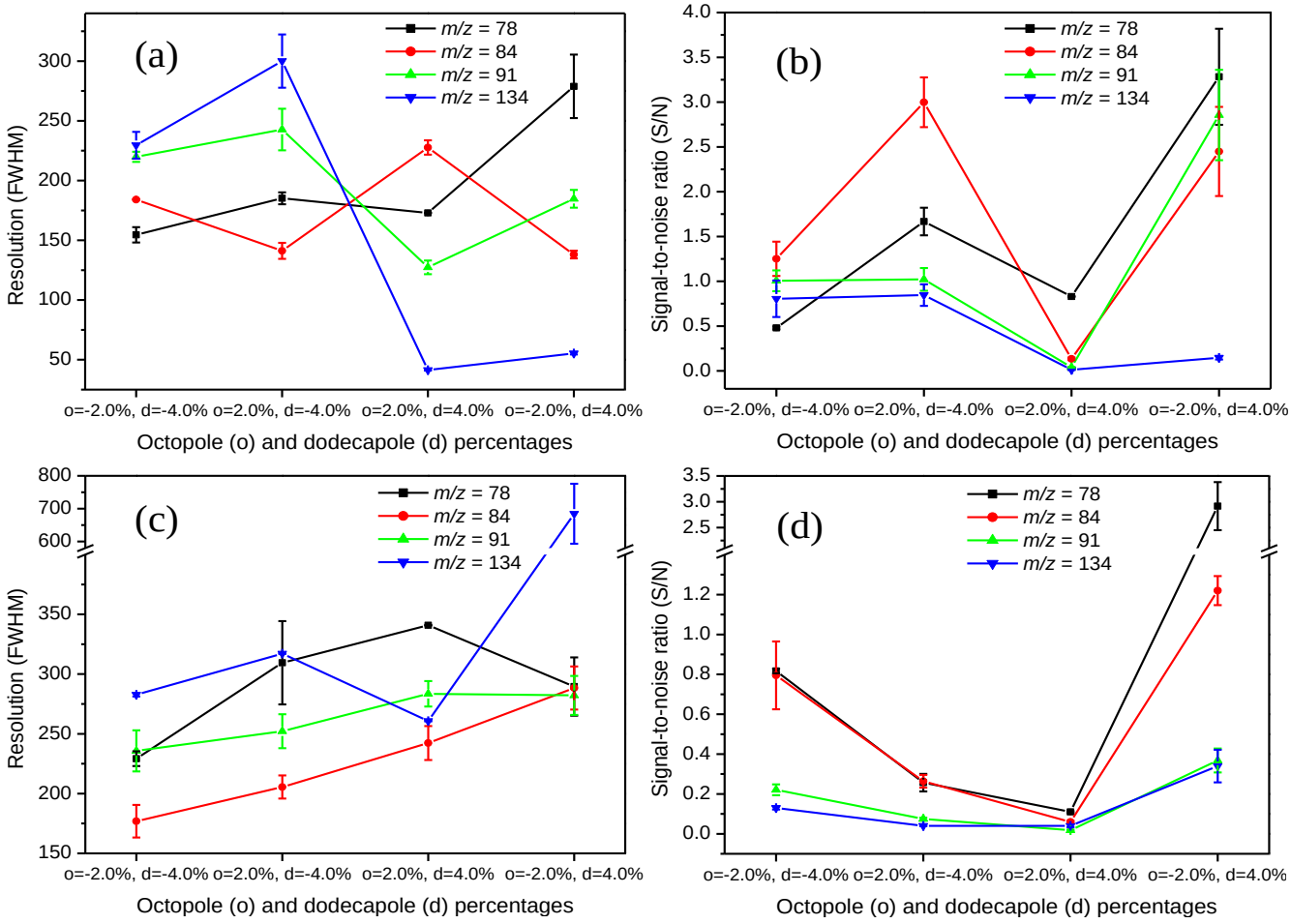
(a)
(b)
(c)
(d)
m/z = 78
m/z = 84
m/z = 91
m/z = 134
Resolution (FWHM)
Signal-to-noise ratio (S/N)
o=-2.0%, d=-4.0%
o=2.0%, d=-4.0%
o=2.0%, d=4.0%
o=-2.0%, d=4.0%
Octopole (o) and dodecapole (d) percentages

Figure 4

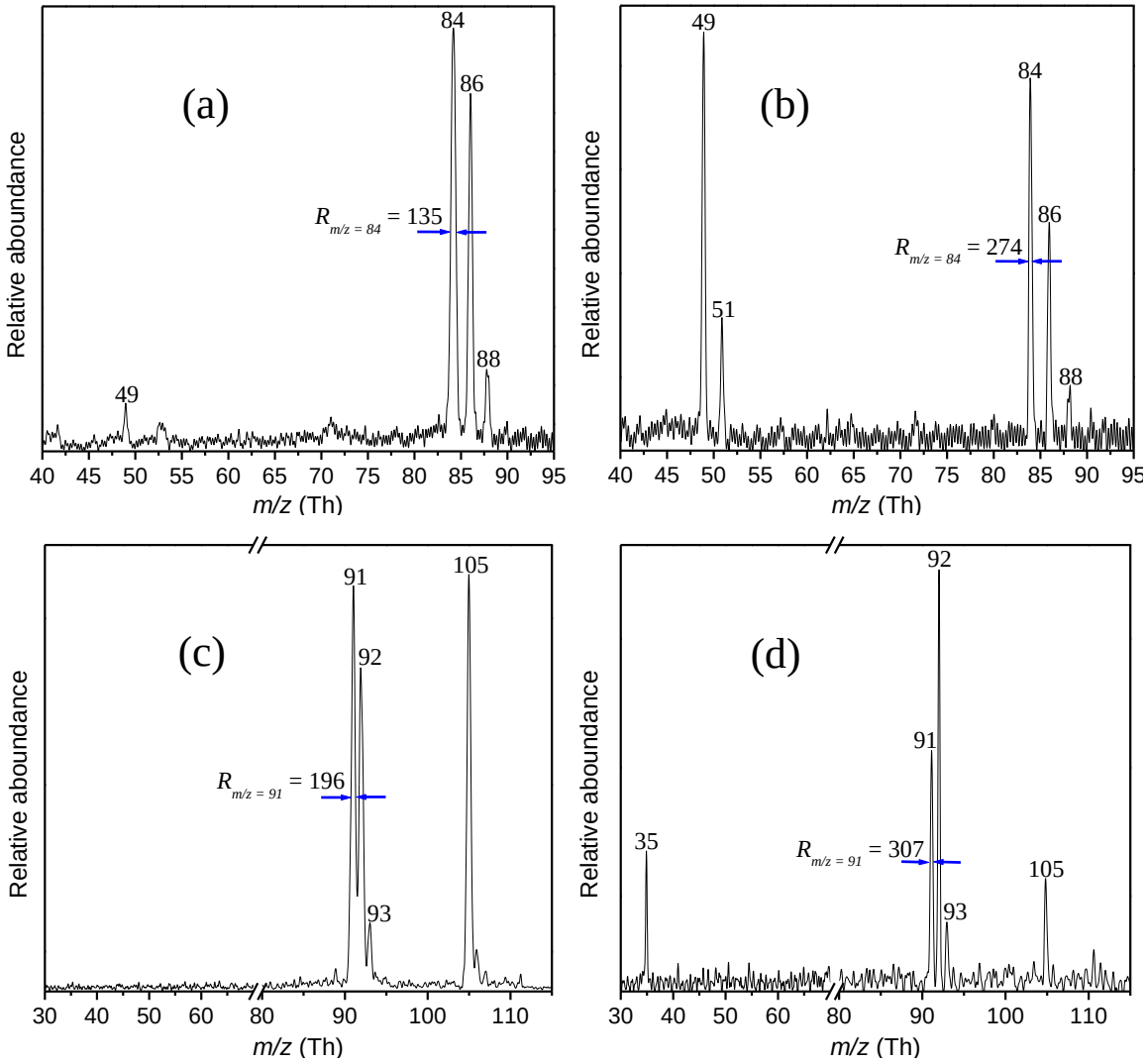
(a)
84
86
88
49
$R_{m/z = 84}$ = 135
Relative abundance
40 45 50 55 60 65 70 75 80 85 90 95
m/z (Th)
(b)
49
84
86
88
51
$R_{m/z = 84}$ = 274
Relative abundance
40 45 50 55 60 65 70 75 80 85 90 95
m/z (Th)
(c)
91
105
92
93
$R_{m/z = 91}$ = 196
Relative abundance
30 40 50 60 80 90 100 110
m/z (Th)
(d)
92
91
35
105
93
$R_{m/z = 91}$ = 307
Relative abundance
30 40 50 60 80 90 100 110
m/z (Th)

Figure 5

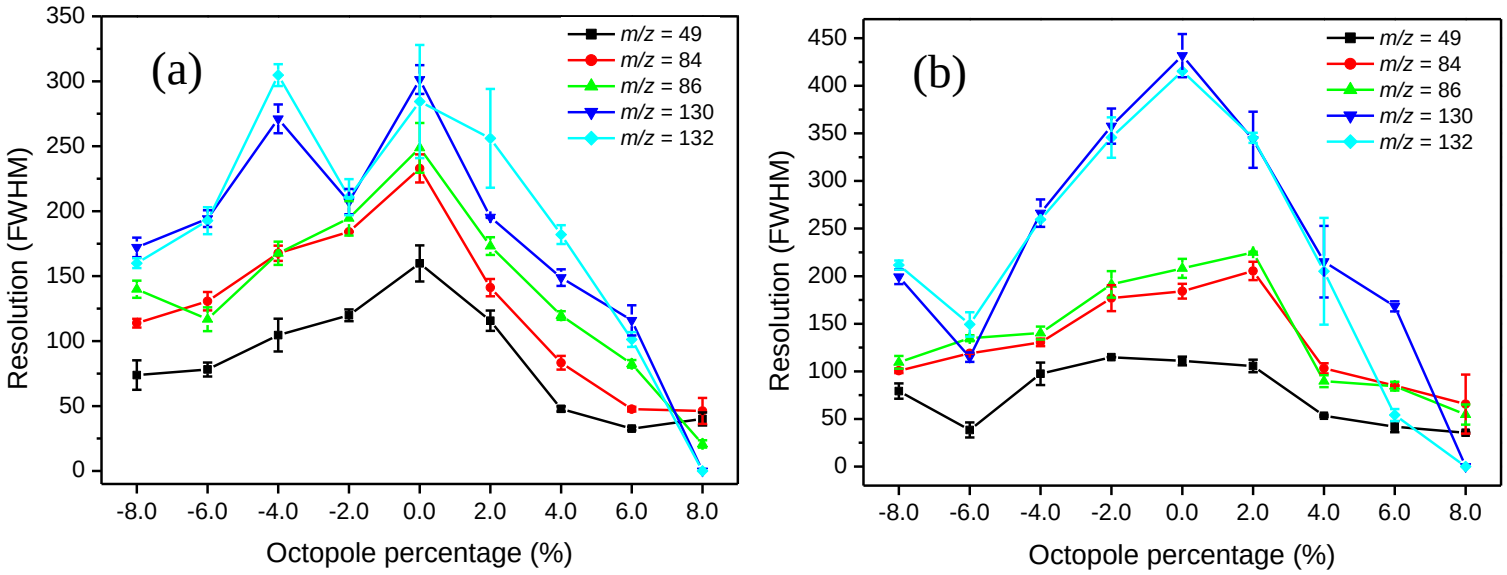

Figure 6

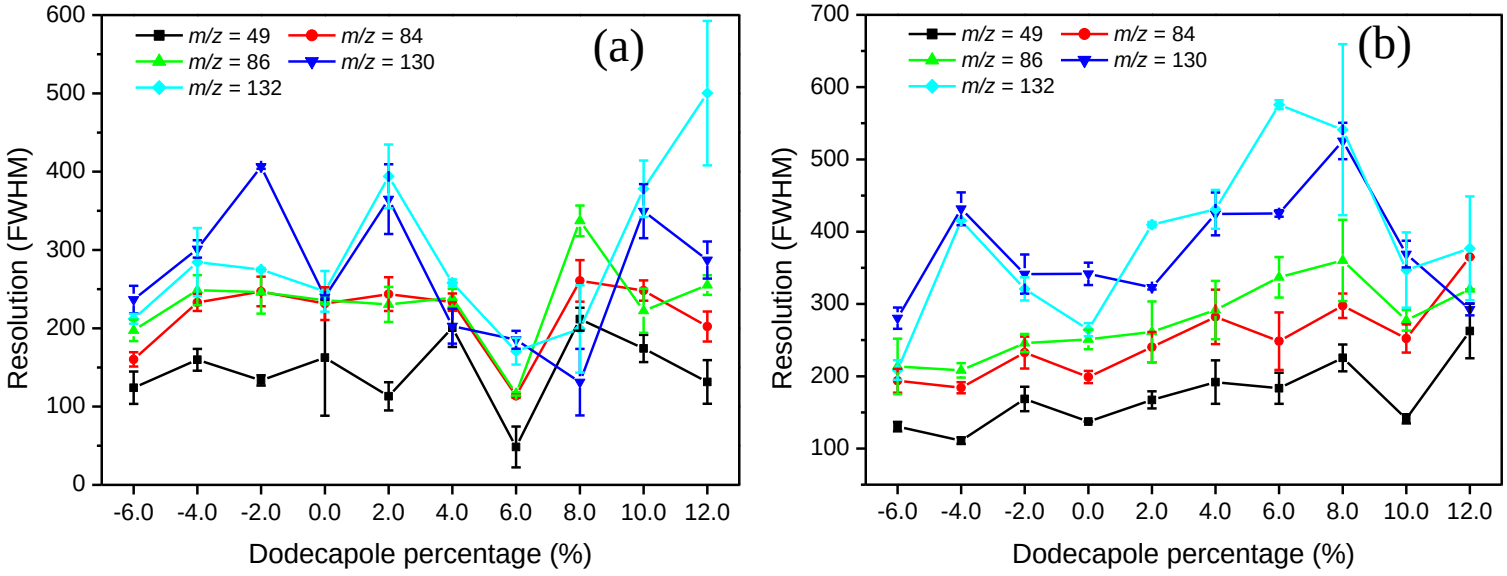

Figure 7

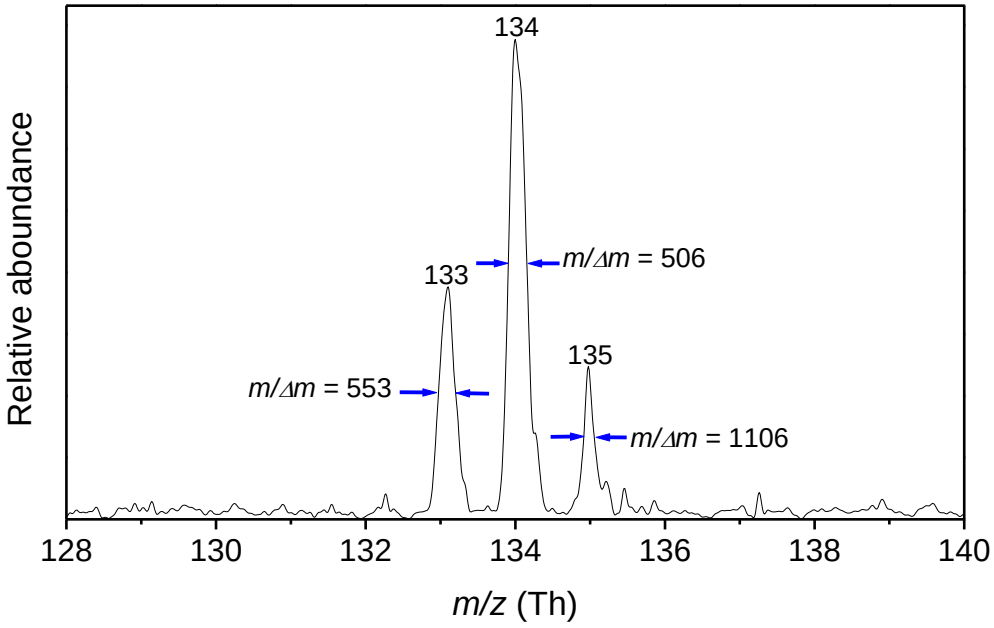
134
133
135
m/Δm = 506
m/Δm = 553
m/Δm = 1106
Relative abundance
128
130
132
134
136
138
140
m/z (Th)

Table 1

Table 1. The relative weights of multipoles including octopole (A_4/A_2), dodecapole (A_6/A_2), hexadecapole (A_8/A_2), ikosipole (A_{10}/A_2), and tetraikosipole (A_{12}/A_2).

No.	A_4/A_2 (%)	A_6/A_2 (%)	A_8/A_2 (%)	A_{10}/A_2 (%)	A_{12}/A_2 (%)
1	8.00	-4.00	-42.23	140.20	-312.51
2	6.00	-4.00	-40.59	136.81	-304.93
3	4.00	-4.00	-38.95	133.41	-297.34
4	2.00	-4.00	-37.12	129.87	-289.56
5	0.00	-4.00	-35.68	126.61	-282.14
6	-2.00	-4.00	-34.05	123.21	-274.53
7	-4.00	-4.00	-32.31	119.77	-267.18
8	-6.00	-4.00	-30.46	116.27	-260.00
9	-8.00	-4.00	-28.66	113.45	-254.91